

# Seismic Passive Earth Pressure Behind Non Vertical Wall with Composite Failure Mechanism: Pseudo-Dynamic Approach

Priyanka Ghosh · Sreevals Kolathayar

Received: 6 January 2010 / Accepted: 24 October 2010 / Published online: 5 November 2010  
© Springer Science+Business Media B.V. 2010

**Abstract** This note shows a study on the seismic passive earth pressure behind a non-vertical cantilever retaining wall using pseudo-dynamic approach. A composite failure surface comprising of an arc of the logarithmic spiral near the wall and a straight line in the planar shear zone near the ground, has been considered behind the retaining wall. The effects of soil friction angle, wall inclination, wall friction angle, amplification of vibration, horizontal and vertical earthquake acceleration on the passive earth pressure have been explored in this study. The results available in the literature for passive pressure, on the basis of pseudo-static analysis are found to predict the passive resistance on the conservative side and the assumption of a planar failure surface is found to overestimate the passive resistance for higher wall friction. An attempt has been made in the present study to overcome both the limitations simultaneously. The present results are compared with the existing values in the literature and found a reasonable match among the values.

**Keywords** Passive earth pressure · Earthquakes · Composite failure · Pseudo-dynamic analysis · Retaining wall

P. Ghosh (✉) · S. Kolathayar  
Department of Civil Engineering, Indian Institute of Technology, Kanpur 208 016, India  
e-mail: priyog@iitk.ac.in

## 1 Introduction

The determination of passive resistance of a retaining wall, under both static and seismic conditions, is very much essential as the damage of such earth retaining structures may lead to significant loss of life and wealth. Several investigations have been performed by different researchers to determine the passive earth pressure on a rigid retaining wall under seismic condition. Okabe (1926) and Mononobe and Matsuo (1929) provided theory to determine the active and passive earth pressure using pseudo-static analysis. This analysis was later recognized as well known Mononobe-Okabe method (Kramer 1996) to compute the seismic earth pressure. The Mononobe-Okabe method incorporates pseudo-static accelerations to the Coulomb's failure wedge to determine the passive earth resistance of cantilever retaining walls, where a planar failure surface was considered. Pseudo-static approach considers the dynamic load induced by an earthquake as time-independent, which ultimately assumes that the magnitude and phase of acceleration are uniform throughout the backfill. To overcome this constraint, Steedman and Zeng (1990) introduced the pseudo-dynamic approach, with a planar failure surface to predict the seismic active earth pressure behind a vertical cantilever retaining wall where the time and phase difference due to finite shear wave velocity were considered. Later Choudhary and Nimbalkar (2005) and Ghosh (2007) also considered the planar failure surface to obtain the passive earth

pressure using pseudo-dynamic approach. Nimbalkar and Choudhury (2008) obtained the effect of body waves and soil amplification on seismic earth pressure using pseudo-dynamic approach. It has been reported by several researchers that the assumption of a planar failure surface overestimates the passive pressures for higher magnitude of wall friction angle. Kumar (2001) used composite failure mechanism for an inclined wall in presence of the horizontal pseudo-static earthquake body force and found that the curved rupture surface results in more acceptable values of passive resistance. Using pseudo-static approach Choudhury and Subba Rao (2002), Choudhury et al. (2004), and Subba Rao and Choudhury (2005) also employed either logarithmic spiral or composite failure mechanism for an inclined retaining wall with inclined backfill to determine the seismic passive earth pressure with both negative and positive wall friction conditions. The consideration of wall inertia effect was considered by Choudhury and Nimbalkar (2007), and Nimbalkar and Choudhury (2007) for sliding and rotational movements of wall for passive cases. For vertical wall, Basha and Babu (2009) adopted pseudo-dynamic approach with a composite failure surface and showed that the pseudo-static method overestimates the passive earth pressure coefficients. However, in the analysis of Basha and Babu (2009), the accelerations of the small radial element inside the logarithmic failure zone were considered same as those at the bottom of the element while carrying out the integration of the inertia forces acting in the logarithmic failure zone and also the magnitude of radial reaction along the logarithmic spiral failure surface was assumed as constant. These assumptions eventually reveal more conservative magnitude of passive resistance. In the present analysis, pseudo-dynamic approach has been considered to obtain the seismic passive earth pressure behind a non-vertical cantilever retaining wall taking the failure surface as a combination of an arc of the logarithmic spiral and a straight line. The present study explores the effects of soil friction angle ( $\phi$ ), angle of inclination of the wall ( $\theta$ ), interface friction angle between the wall backface and soil medium ( $\delta$ ), horizontal earthquake acceleration coefficient ( $\alpha_h$ ), vertical earthquake acceleration coefficient ( $\alpha_v$ ), amplification factor ( $f_a$ ), shear wave velocity ( $V_s$ ) and primary wave velocity ( $V_p$ ) on the seismic passive earth pressure using the pseudo-dynamic approach.

## 2 Definition of the Problem

A rigid non-vertical cantilever retaining wall of height  $H$  is placed with a dry, cohesionless, horizontal backfill as shown in Fig. 1a. The wall face (AB) on the backfill side is inclined at an angle  $\theta$  with the vertical and has a wall friction angle  $\delta$ . The objective is to determine the passive earth resistance  $P_{pe}$  in the presence of a sinusoidal base shaking subjected to linearly varying horizontal and vertical accelerations with amplitudes of  $\left[1 + (f_a - 1)\frac{(H-z)}{H}\right]\alpha_h g$  and  $\left[1 + (f_a - 1)\frac{(H-z)}{H}\right]\alpha_v g$ , respectively, where  $z$  is any depth below the ground surface and  $g$  is the acceleration due to gravity. The parameters shown in Fig. 1 are considered as positive and the unit weight of the soil is taken as  $\gamma$ .

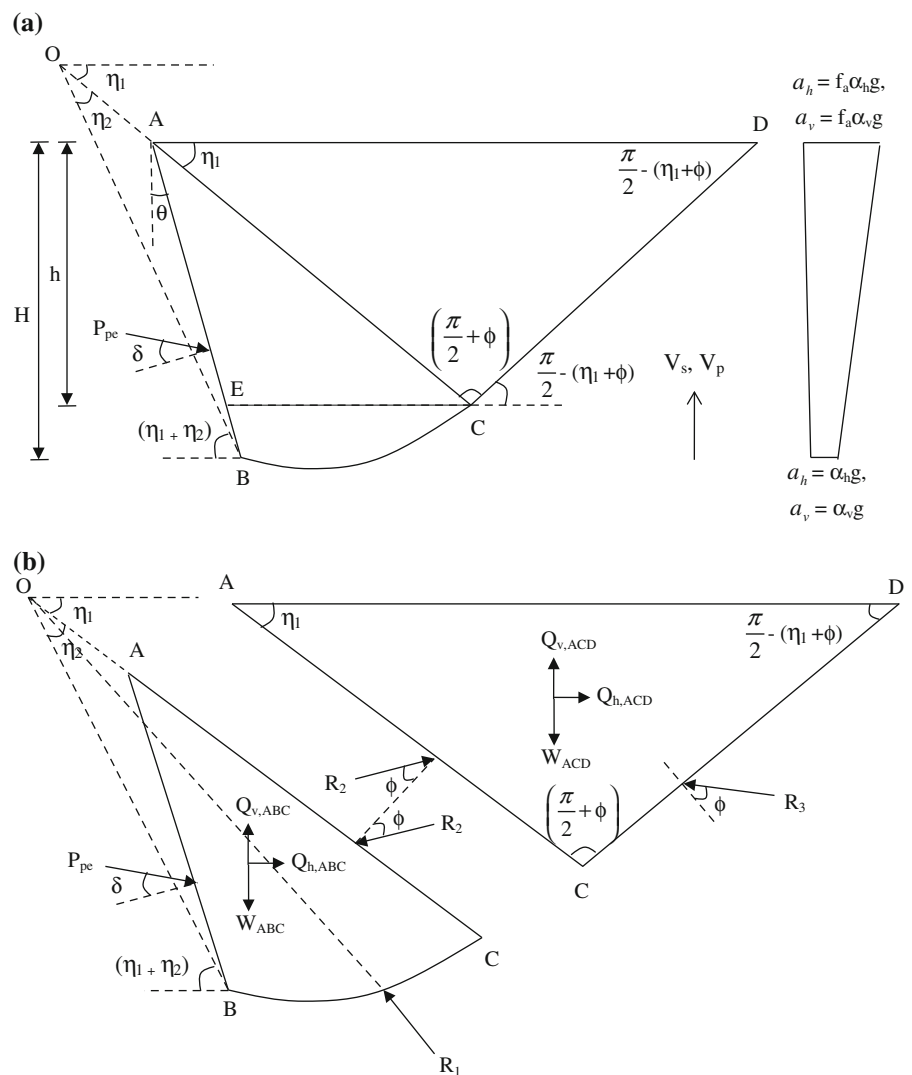
## 3 Assumptions

- The shear modulus ( $G$ ) of the soil medium is constant with depth.
- The nature of amplification depends on many factors such as stiffness and damping of the soil mass, the depth of soil layer, geometry and rigidity of adjacent structures. However, a simplified linear variation of amplification of vibration is considered. This consideration of amplification is in accordance with the finding of Nimbalkar and Choudhury (2008).
- The point of application of the interface reaction ( $R_2$ ) between the planar and logarithmic spiral failure zone and passive resistance ( $P_{pe}$ ) is considered at the bottom third of the plane on which they act.

## 4 Analysis

A composite failure surface BCD (Fig. 1a) defined by the angles  $\eta_1$  and  $\eta_2$  has been considered in the analysis. The failure surface is assumed to be of a composite shape comprising of an arc of the logarithmic spiral near the wall and a straight line in the planar shear zone near the ground. In order that the arc of the logarithmic spiral joins tangentially with the straight failure surface in the planar shear zone, and also that the planar shear zone exists near the ground; the focus (O) of the logarithmic spiral

**Fig. 1** Failure mechanism and associated forces



must lie on the straight line (OC) passing through the top of the wall (A) and inclined at an angle  $\eta_1$  with the horizontal, where  $\eta_1$  has been optimized to get the minimum value of passive resistance. The passive thrust,  $P_{pe}$  makes an angle,  $\delta$  with the normal to the wall face (AB). The failure mechanism has then been solved using pseudo-dynamic approach to compute the passive resistance.

The pseudo-dynamic analysis, which considers finite shear and primary wave velocities, can be developed by assuming constant shear modulus  $G$  throughout the backfill and thus creating the variation in phase not in magnitude of the horizontal and vertical accelerations. The present analysis considers both shear and primary wave velocities

acting within the backfill during the earthquake in the direction as shown in Fig. 1a. The analysis includes a period of lateral shaking  $T$  and therefore, the horizontal and vertical accelerations at any depth  $z$  below the ground surface and time  $t$  can be given by

$$a_h(z, t) = \alpha_h g \left[ 1 + (f_a - 1) \frac{(H-z)}{H} \right] \sin \omega \left( t - \frac{H-z}{V_s} \right) \quad (1)$$

$$a_v(z, t) = \alpha_v g \left[ 1 + (f_a - 1) \frac{(H-z)}{H} \right] \sin \omega \left( t - \frac{H-z}{V_p} \right) \quad (2)$$

These equations are similar to those mentioned by Nimbalkar and Choudhury (2008).

#### 4.1 Derivation of Forces in the Wedge ACD

The mass of the small shaded part of thickness  $dz$  in the failure wedge ACD (Fig. 2a) is given by

$$m_{ACD}(z) = \frac{\gamma}{g} \{(h-z) \cot \eta_1 + (h-z) \tan(\eta_1 + \phi)\} dz \quad (3)$$

where,  $h$  is the vertical depth of the planar shear zone ACD as shown in Fig. 1a.

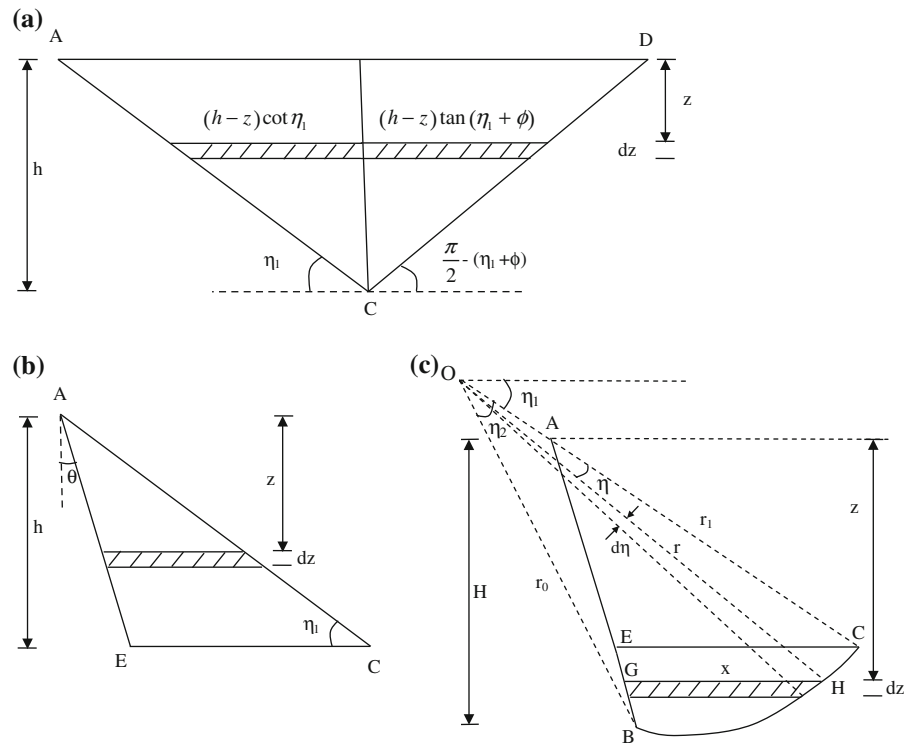
The total weight of the wedge ( $W_{ACD}$ ) can then be derived from Eq. (3) and is given by

$$W_{ACD} = \frac{1}{2} \gamma h^2 (\cot \eta_1 + \tan(\eta_1 + \phi)) \quad (4)$$

The inertia force exerted on the small element due to the horizontal earthquake acceleration can be expressed as  $m_{ACD}(z)a_h(z, t)$ . Therefore, the total horizontal inertia force  $Q_{ACD,h}$  acting in the wedge ACD is given by

$$Q_{ACD,h}(t) = \gamma \int_0^{H_1} \{(h-z) \cot \eta_1 + (h-z) \tan(\eta_1 + \phi)\} \times \alpha_h \left[ 1 + \frac{(H-z)}{H} (f_a - 1) \right] \sin \omega \left( t - \frac{H-z}{V_s} \right) dz \quad (5)$$

**Fig. 2** Methodology to obtain the associated forces



Similarly, the total vertical inertia force  $Q_{ACD,v}$  acting in the wedge ACD is given by

$$Q_{ACD,v}(t) = \gamma \int_0^{H_1} \{(h-z) \cot \eta_1 + (h-z) \tan(\eta_1 + \phi)\} \times \alpha_v \left[ 1 + \frac{(H-z)}{H} (f_a - 1) \right] \sin \omega \left( t - \frac{H-z}{V_p} \right) dz \quad (6)$$

Considering the horizontal and vertical force equilibrium in the wedge ACD, the reaction  $R_2$  can be obtained as

$$R_2(t) = \frac{(W_{ACD} - Q_{ACD,h} \tan \eta_1 - Q_{ACD,v})}{(\cos(\eta_1 + \phi) + \sin(\eta_1 + \phi) \tan \eta_1)} \quad (7)$$

It is important to note here that the force  $R_2$  acts at the interface between logarithmic and planar failure zone and in the present analysis, the point of application of  $R_2$  is assumed at one-third of AC from point C.

#### 4.2 Moment of Forces Acting in the Wedge AEC About O

The mass of the small shaded part of thickness  $dz$  in the wedge AEC (Fig. 2b) is given by

$$m_{AEC}(z) = \frac{\gamma}{g} z (\cot \eta_1 - \tan \theta) dz \quad (8)$$

The total weight of the wedge ( $W_{AEC}$ ) can then be expressed as

$$W_{AEC} = \frac{1}{2} \gamma h^2 \frac{\cos(\eta_1 + \theta)}{\sin \eta_1 \cos \theta} \quad (9)$$

The total horizontal and vertical inertia forces acting in the wedge AEC can be expressed as

$$Q_{AEC,h}(t) = \gamma \int_0^{H_1} z (\cot \eta_1 - \tan \theta) \alpha_h \times \left[ 1 + \frac{(H-z)}{H} (f_a - 1) \right] \sin \omega \left( t - \frac{H-z}{V_s} \right) dz \quad (10)$$

$$Q_{AEC,v}(t) = \gamma \int_0^{H_1} z (\cot \eta_1 - \tan \theta) \alpha_v \times \left[ 1 + \frac{(H-z)}{H} (f_a - 1) \right] \sin \omega \left( t - \frac{H-z}{V_p} \right) dz \quad (11)$$

The moment of all the forces acting in the wedge AEC with respect to the focus (O) of logarithmic spiral failure surface can be expressed as

$$M_{AEC}(t) = \frac{1}{3} (W_{AEC} - Q_{AEC,v}) \times ((2l + r_1) \cos \eta_1 + h \tan \theta) - \frac{1}{3} [Q_{AEC,h} \times (l + 2r_1) \sin \eta_1 + R_2 \cos \phi \times (2r_1 + l)] \quad (12)$$

where,  $l$  is the distance from the top of wall to the focus (O) of logarithmic spiral failure surface (BC) and  $r_1$  is the final radius of the logarithmic spiral surface (BC).

#### 4.3 Moment of Forces Acting in the Wedge EBC About O

To overcome the conservative assumption of Basha and Babu (2009) regarding the accelerations in the radial strip, an elemental horizontal strip of thickness  $dz$  has been considered in the wedge EBC (Fig. 2c) at a depth  $z$  from the ground surface which can be defined by an angle  $\eta$ . At any angle  $\eta$ , the radius (OH) of the logarithmic spiral can be expressed as  $r = r_0 e^{(\eta_2 - \eta) \tan \phi}$ , where  $r_0$  is the initial radius of the logarithmic spiral failure surface.

The moments due to the weight, horizontal and vertical inertia forces acting in the whole wedge EBC about O can be obtained by integrating the moments of respective forces in the elemental strip with respect to  $\eta$  varying from 0 to  $\eta_2$  and their expressions can be written as

$$M_{EBC,w} = \gamma \int_0^{\eta_2} x \left( r \cos(\eta_1 + \eta) - \frac{x}{2} \right) r \{ \cos(\eta_1 + \eta) - \sin(\eta_1 + \eta) \tan \phi \} d\eta \quad (13)$$

$$M_{EBC,h}(t) = \gamma \int_0^{\eta_2} x \alpha_h \left[ 1 + \frac{(H-z)}{H} (f_a - 1) \right] \times \sin \omega \left( t - \frac{H-z}{V_s} \right) r \sin(\eta_1 + \eta) r \{ \cos(\eta_1 + \eta) - \sin(\eta_1 + \eta) \tan \phi \} d\eta \quad (14)$$

$$M_{EBC,v}(t) = \gamma \int_0^{\eta_2} x \alpha_v \left[ 1 + \frac{(H-z)}{H} (f_a - 1) \right] \times \sin \omega \left( t - \frac{H-z}{V_p} \right) \left( r \cos(\eta_1 + \eta) - \frac{x}{2} \right) \times r \{ \cos(\eta_1 + \eta) - \sin(\eta_1 + \eta) \tan \phi \} d\eta \quad (15)$$

where,  $x$  is the horizontal length of the strip GH as shown in Fig. 2c. It is worth mentioning here that the resultant force ( $R_1$ ) of the normal and shear forces along the logarithmic spiral failure surface does not contribute any moment about O as  $R_1$  passes through the focus (O) following the properties of the logarithmic spiral. The resultant moment acting in the wedge EBC is therefore, given by

$$M_{EBC}(t) = M_{EBC,w} - M_{EBC,h} - M_{EBC,v} \quad (16)$$

#### 4.4 Estimation of Passive Earth Resistance

The total moment about point O; caused by the weight, horizontal and vertical inertia forces acting in the wedge ABC can be expressed as

$$M_{ABC}(t) = M_{AEC} + M_{EBC} \quad (17)$$

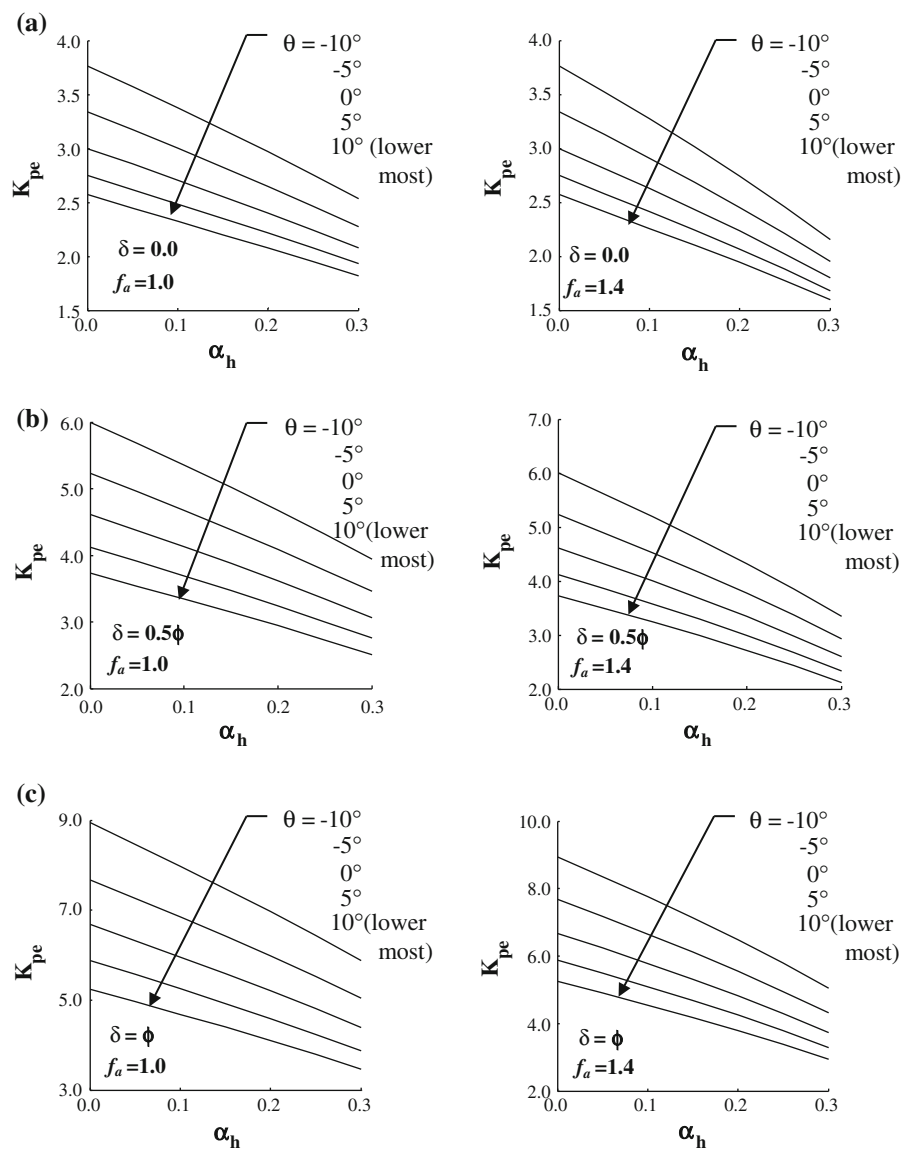
It is assumed that the point of application of the passive resistance lies at the bottom third of the wall, which is found reasonable for lower values of  $H/TV_s$  as observed by Steedman and Zeng (1990). Hence, the total passive resistance  $P_{pe}$  can be determined by

taking the moment equilibrium of the whole wedge ABC about the point O and is given by

The seismic passive earth pressure coefficient can then be obtained as

$$P_{pe}(t) = \frac{M_{ABC}}{\cos(\delta - \theta)(\frac{2}{3}H + l \sin \eta_1) - \sin(\delta - \theta)(\frac{2}{3}H \tan \theta + l \cos \eta_1)} \quad (18)$$

**Fig. 3** Variation of passive pressure coefficient  $K_{pe}$  with  $\alpha_h$  for  $\phi = 30^\circ$ ,  $\alpha_v = 0.5\alpha_h$ ,  $H/TV_s = 0.3$  and  $H/TV_p = 0.16$ .  
**a**  $\delta = 0.0$ ; **b**  $\delta = 0.5\phi$ ; **c**  $\delta = \phi$



$$K_{pe}(t) = \frac{2P_{pe}}{\gamma H^2} \quad (19)$$

It can be observed that  $K_{pe}$  is a function of  $\eta_1$ ,  $\eta_2$ ,  $H/TV_s$  and  $H/TV_p$ . The optimization has been performed with respect to  $\eta_1$ ,  $\eta_2$  and  $t/T$  to obtain the minimum value of  $K_{pe}$ . During optimization, the values of  $\eta_1$ ,  $\eta_2$  and  $t/T$  have been varied in the range of 0 to  $(90 - \phi)$ , 0 to  $(90 - \eta_1 - \theta)$  and 0–1, respectively.

## 5 Results

The computations have been performed by writing a computer code in MATLAB. To find out the minimum value of  $K_{pe}$ , the magnitude of the variables  $\eta_1$ ,  $\eta_2$  and  $t/T$  has been varied independently at an interval of  $1^\circ$ ,  $1^\circ$  and 0.1, respectively.

The variation of seismic passive earth pressure coefficient  $K_{pe}$  with changes in  $\alpha_h$  for different values of  $\theta$ ,  $\delta$  and  $f_a$  are presented in Fig. 3 for  $\phi = 30^\circ$ ,  $\alpha_v = 0.5\alpha_h$ ,  $H/TV_s = 0.3$  and  $H/TV_p = 0.16$ . The values of  $K_{pe}$  are also presented in Table 1 for  $\phi = 40^\circ$ ,  $\alpha_v = 0.5\alpha_h$ ,  $f_a = 1.4$ ,  $H/TV_s = 0.3$  and  $H/TV_p = 0.16$ . It can be seen that the magnitude of passive earth pressure coefficient decreases continuously with an increase in the magnitude of  $\alpha_h$ . It can also be observed that the value of  $K_{pe}$  decreases with increase in the wall inclination  $\theta$  from negative to positive. It is important to mention here that the magnitude of  $\theta$  becomes positive or negative when the wall face rotates in the anti-clockwise or

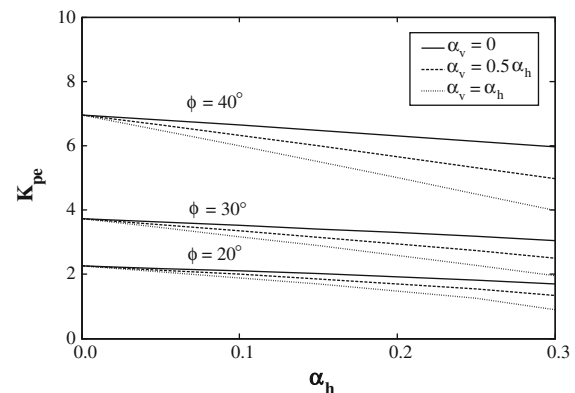


**Fig. 4** Variation of passive pressure coefficient with  $\alpha_h$  for different values of  $\phi$  and  $\alpha_v$  ( $\theta = 0^\circ$ ,  $\delta = 0.5\phi$ ,  $H/TV_s = 0.3$ ,  $H/TV_p = 0.16$ )

clockwise direction from the vertical, respectively. Therefore, the uppermost line in Fig. 3 indicates  $\theta = -10^\circ$ ; whereas the lowermost line is for  $\theta = 10^\circ$ . The value of  $K_{pe}$  also increases with increase in the magnitude of  $\delta$ . It has been seen that higher the amplification factor  $f_a$ , the lesser is the magnitude of  $K_{pe}$ .

The variations of  $K_{pe}$  with changes in  $\alpha_h$  for different values of  $\phi$  and  $\alpha_v$  are presented in Fig. 4 with  $\theta = 0^\circ$ ,  $\delta = 0.5\phi$ ,  $H/TV_s = 0.3$  and  $H/TV_p = 0.16$ . It can be noticed that the values of  $K_{pe}$  continuously decrease with increase in the magnitude of  $\alpha_h$  and  $\alpha_v$ . It is worthy to observe here that the reduction in the magnitude of  $K_{pe}$  with increase in  $\alpha_h$  becomes higher as the magnitude of  $\alpha_v$  increases.

## 6 Comparison

In absence of vertical seismic force and amplification of accelerations ( $\alpha_v = 0$  and  $f_a = 1.0$ ), the comparison of present values of passive earth pressure coefficient with the values given by Soubra (2000), Kumar (2001), Choudhary and Nimbalkar (2005), Subba Rao and Choudhury (2005), Ghosh (2007), and Basha and Babu (2009) for a vertical wall ( $\theta = 0^\circ$ ) are presented in Table 2. A comparison of passive earth pressure coefficient is also shown in Fig. 5 for  $\phi = 30^\circ$ ,  $\delta = 2\phi/3$ ,  $\theta = 0^\circ$ ,  $\alpha_v = 0$ ,  $f_a = 1.0$ ,  $H/TV_s = 0.3$  and  $H/TV_p = 0.16$ . The values predicted by Kumar (2001) are slightly lower than the present values for lower values of  $\alpha_h$ ; whereas the difference

**Table 1** Values of passive earth pressure coefficient  $K_{pe}$  for  $\phi = 40^\circ$ ,  $\alpha_v = 0.5\alpha_h$ ,  $f_a = 1.4$ ,  $H/TV_s = 0.3$ ,  $H/TV_p = 0.16$

$\delta$	$\alpha_h$	$K_{pe}$				
		$\theta = -10^\circ$	$\theta = -5^\circ$	$\theta = 0^\circ$	$\theta = 5^\circ$	$\theta = 10^\circ$
$0.0$	0.0	6.36	5.37	4.60	4.05	3.67
	0.2	4.86	4.12	3.56	3.16	2.86
	0.4	3.16	2.73	2.42	2.19	2.02
	$0.5\phi$	14.28	11.66	9.67	8.15	6.96
	0.2	10.87	8.87	7.36	6.20	5.31
	0.4	7.03	5.72	4.75	4.01	3.44
$\phi$	0.0	29.00	23.22	18.87	15.55	12.99
	0.2	22.62	17.97	14.52	11.92	9.93
	0.4	15.36	12.01	9.58	7.80	6.46

**Table 2** Comparison of passive earth pressure coefficient  $K_{pe}$  for  $\phi = 30^\circ$ ,  $\theta = 0^\circ$ ,  $\alpha_v = 0$ ,  $f_a = 1.0$ ,  $H/TV_s = 0.3$  and  $H/TV_p = 0.16$ 

$\delta$	$\alpha_h$	$K_{pe}$						
		Present analysis	Soubra (2000)	Kumar (2001)	Choudhary and Nimbalkar (2005)	Subba Rao and Choudhury (2005)	Ghosh (2007)	Basha and Babu (2009)
0	0.00	3.00	3.00	3.00	3.00	—	3.00	3.00
	0.05	2.92	2.91	2.92	2.92	—	2.92	2.87
	0.10	2.85	2.82	2.82	2.85	—	2.85	2.75
	0.15	2.77	2.73	2.72	2.77	—	2.77	2.61
	0.20	2.68	2.63	2.62	2.68	—	2.68	2.44
	0.25	2.60	2.53	2.51	2.60	—	2.60	2.28
	0.30	2.51	2.42	2.39	2.51	—	2.51	2.11
$\phi/3$	0.00	4.02	4.05	4.02	4.14	—	4.14	4.03
	0.05	3.91	3.91	3.89	4.01	—	4.01	3.74
	0.10	3.79	3.77	3.75	3.87	—	3.87	3.60
	0.15	3.67	3.62	3.61	3.73	—	3.73	3.46
	0.20	3.54	3.47	3.46	3.59	—	3.59	3.30
	0.25	3.41	3.31	3.30	3.45	—	3.45	3.07
	0.30	3.27	3.13	3.13	3.29	—	3.29	2.85
$2\phi/3$	0.00	5.26	5.40	5.26	6.11	—	6.11	5.25
	0.05	5.10	5.20	5.08	5.87	—	5.87	4.69
	0.10	4.94	5.00	4.89	5.63	—	5.63	4.40
	0.15	4.78	4.79	4.69	5.38	—	5.38	4.10
	0.20	4.60	4.57	4.48	5.14	—	5.14	3.75
	0.25	4.42	4.34	4.27	4.88	—	4.88	3.46
	0.30	4.23	4.10	4.03	4.63	—	4.63	3.00
$\phi$	0.00	6.68	6.86	6.68	10.10	5.78	10.10	6.60
	0.05	6.47	6.61	6.44	9.64	5.67	9.64	6.02
	0.10	6.26	6.35	6.19	9.17	5.40	9.17	5.60
	0.15	6.05	6.07	5.93	8.70	5.33	8.70	5.08
	0.20	5.82	5.79	5.66	8.23	5.10	8.23	4.48
	0.25	5.59	5.49	5.37	7.75	5.00	7.75	3.88
	0.30	5.34	5.17	5.07	7.26	4.75	7.26	3.40

increases for higher values of  $\alpha_h$  and  $\delta$ . This difference occurs due to the pseudo-static approach adopted by Kumar (2001), which does not consider the effect of time and phase difference due to finite shear wave velocity and therefore predicts the conservative results; whereas the present analysis incorporates the pseudo-dynamic approach. For a vertical wall with zero wall friction ( $\delta = 0^\circ$  and  $\theta = 0^\circ$ ), the present values are in line with those reported by Choudhary and Nimbalkar (2005), and Ghosh (2007), which implies that the logarithmic

spiral part of the failure surface disappears for a smooth vertical wall; whereas for higher values of wall friction, the assumption of composite failure surface gives more reasonable values of  $K_{pe}$  which are much lesser than those predicted using a planar failure surface. It can be seen that the values of  $K_{pe}$  given by Basha and Babu (2009) are much lower than the values predicted by the present analysis, Soubra (2000) and Kumar (2001). The significant difference between the results of Basha and Babu (2009), and the present analysis might be caused due to the

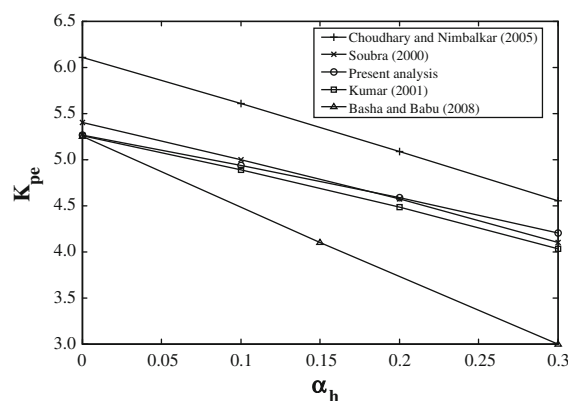


**Fig. 5** Comparison of passive earth pressure coefficient  $K_{pe}$  for  $\phi = 30^\circ$ ,  $\delta = 2\phi/3$ ,  $\theta = 0^\circ$ ,  $\alpha_v = 0$ ,  $f_a = 1.0$ ,  $H/TV_s = 0.3$  and  $H/TV_p = 0.16$

assumption of constant magnitude of radial reaction along the logarithmic spiral failure surface as well as the conservative consideration of accelerations inside the logarithmic failure zone.

The comparison of present values of passive earth pressure coefficient with the values given by Chang (1981), Soubra (2000), Kumar (2001), Choudhary and Nimbalkar (2005), Subba Rao and Choudhury

(2005), Ghosh (2007) and Lancellotta (2007) are shown in Table 3 for  $\theta = 0^\circ$ ,  $\delta = 0.5\phi$ ,  $\alpha_v = 0$ ,  $f_a = 1.0$ ,  $H/TV_s = 0.3$  and  $H/TV_p = 0.16$ . Being a lower-bound solution the values obtained by Lancellotta (2007) are found to be the lowest; whereas the values of Choudhary and Nimbalkar (2005), and Ghosh (2007) are found to be higher due to the assumption of a planar failure surface. However, the present values match reasonably well with the values given by Chang (1981), Soubra (2000), Kumar (2001), and Subba Rao and Choudhury (2005).

For  $\alpha_v = 0$  and  $f_a = 1.0$ , the comparison of present values of passive earth pressure coefficient with the values obtained by Mononobe-Okabe method, Kumar (2001), Kumar and Chitikela (2002), and Ghosh (2007) are given in Tables 4 and 5 for  $\theta = -15$  and  $15^\circ$ , respectively. It is worth mentioning here that according to Kumar (2001), the shape of the proposed logarithmic failure surface shifts gradually from convex to concave for a combination of lower values of  $\delta$  and higher values of  $\theta$  (positive). In such cases, the assumption of a convex failure surface, as in the present analysis, slightly overestimates the passive pressure coefficient as seen in Table 5.

**Table 3** Comparison of passive earth pressure coefficient  $K_{pe}$  for  $\theta = 0^\circ$ ,  $\delta = 0.5\phi$ ,  $\alpha_v = 0$ ,  $f_a = 1.0$ ,  $H/TV_s = 0.3$  and  $H/TV_p = 0.16$

$\phi$	$\alpha_h$	$K_{pe}$							
		Present analysis	Chang (1981)	Soubra (2000)	Kumar (2001)	Choudhary and Nimbalkar (2005)	Subba Rao and Choudhury (2005)	Ghosh (2007)	Lancellotta (2007)
25°	0.0	3.39	3.45	3.43	3.39	3.55	—	3.55	3.10
	0.1	3.17	2.89	3.15	3.13	3.26	—	3.26	2.86
	0.2	2.92	2.74	2.85	2.84	2.96	—	2.96	2.62
	0.3	2.65	2.38	2.50	2.49	2.63	—	2.63	2.26
30°	0.0	4.61	4.64	4.69	4.61	4.98	4.44	4.98	4.29
	0.1	4.34	4.29	4.35	4.30	4.60	4.22	4.60	3.93
	0.2	4.05	3.93	3.99	3.95	4.21	3.89	4.21	3.57
	0.3	3.73	3.45	3.59	3.56	3.80	3.44	3.80	3.21
35°	0.0	6.52	6.67	6.67	6.52	7.36	—	7.36	5.71
	0.1	6.17	6.19	6.24	6.12	6.84	—	6.84	5.48
	0.2	5.81	5.71	5.78	5.68	6.31	—	6.31	5.00
	0.3	5.42	5.24	5.29	5.22	5.76	—	5.76	4.52
40°	0.0	9.67	10.00	9.99	9.67	11.77	9.00	11.77	8.33
	0.1	9.21	9.29	9.40	9.13	11.00	8.78	11.00	7.86
	0.2	8.73	8.57	8.79	8.56	10.21	8.44	10.21	7.26
	0.3	8.22	8.10	8.15	7.96	9.41	8.22	9.41	6.67

**Table 4** Comparison of passive earth pressure coefficient  $K_{pe}$  for  $\theta = -15^\circ$ ,  $\alpha_v = 0$ ,  $f_a = 1.0$ ,  $H/TV_s = 0.3$  and  $H/TV_p = 0.16$

$\phi$	$\delta$	$\alpha_h$	$K_{pe}$				
			Present analysis	Mononobe-Okabe method	Kumar (2001)	Kumar and Chitikela (2002)	Ghosh (2007)
$30^\circ$	0	0.0	4.30	4.45	4.30	4.29	4.45
		0.2	3.78	3.74	3.69	3.68	3.84
		0.4	3.17	2.93	2.93	2.92	3.17
	$\phi$	0.0	10.56	34.06	10.56	10.24	34.06
		0.2	9.19	25.02	8.87	8.60	26.26
		0.4	7.56	15.61	6.79	6.60	18.23
	40°	0	7.68	8.15	7.68	7.66	8.15
		0.2	6.94	7.09	6.81	6.80	7.24
		0.4	6.13	5.97	5.85	5.84	6.29
	$\phi$	0.0	36.76	—	36.76	34.59	—
		0.2	33.47	—	32.26	30.35	—
		0.4	29.80	—	27.23	25.64	—

**Table 5** Comparison of passive earth pressure coefficient  $K_{pe}$  for  $\theta = 15^\circ$ ,  $\alpha_v = 0$ ,  $f_a = 1.0$ ,  $H/TV_s = 0.3$  and  $H/TV_p = 0.16$

$\phi$	$\delta$	$\alpha_h$	$K_{pe}$				
			Present analysis	Mononobe-Okabe method	Kumar (2001)	Kumar and Chitikela (2002)	Ghosh (2007)
$30^\circ$	0	0.0	2.45	2.38	2.34	2.30	2.38
		0.2	2.21	2.16	2.08	2.00	2.19
		0.4	1.95	1.86	1.73	1.61	1.92
	$\phi$	0.0	4.73	5.46	4.73	4.69	5.46
		0.2	4.15	4.48	4.04	4.01	4.58
		0.4	3.46	3.38	3.18	3.16	3.61
	40°	0	3.40	3.26	3.17	3.07	3.26
		0.2	3.13	3.04	2.91	2.77	3.06
		0.4	2.86	2.77	2.59	2.42	2.82
	$\phi$	0.0	11.01	17.37	11.01	10.8	17.37
		0.2	9.94	14.57	9.74	9.57	14.84
		0.4	8.76	11.68	8.31	8.18	12.24

In the presence of seismic vertical force, the comparison of the present values of  $K_{pe}$  with the values given by Mononobe-Okabe method and Ghosh (2007) are presented in Table 6 for  $\theta = -5^\circ$ . It can be seen that the present values of  $K_{pe}$  match quite well with the values obtained by Mononobe-Okabe method and Ghosh (2007) for lower values of  $\phi$  and  $\delta$ ; whereas for higher values of  $\phi$  and  $\delta$ , the present values differ and the difference increases with increase in  $\phi$  and  $\delta$ . This difference arises due to the application of planar failure surface by Mononobe-Okabe method and Ghosh (2007), whereas the present analysis considers a composite failure surface.

## 7 Conclusion

Using the pseudo-dynamic analysis and with the assumption of composite failure surface, the effects of soil friction angle, wall inclination, wall friction angle, horizontal and vertical earthquake acceleration, amplification of vibration, and shear and primary wave velocity on the total seismic passive earth pressure behind a non-vertical cantilever retaining wall have been determined. Both positive and negative wall inclinations have been considered and it is found that the magnitude of seismic passive earth pressure decreases with increase in the values of wall

**Table 6** Comparison of passive earth pressure coefficient  $K_{pe}$  for  $\theta = -5^\circ$ ,  $\alpha_v = 0.5\alpha_h$ ,  $f_a = 1.0$ ,  $H/TV_s = 0.3$  and  $H/TV_p = 0.16$ 

$\phi$	$\delta$	$\alpha_h$	$K_{pe}$ Present analysis	Mononobe- Okabe method	Ghosh (2007)
20°	0	0.0	2.18	2.19	2.19
		0.1	1.94	1.90	1.93
		0.2	1.66	1.58	1.66
	0.5 $\phi$	0.0	2.77	2.91	2.91
		0.1	2.43	2.46	2.51
		0.2	2.06	1.97	2.08
	$\phi$	0.0	3.35	4.04	4.04
		0.1	2.93	3.33	3.41
		0.2	2.46	2.57	2.74
30°	0	0.0	3.34	3.35	3.35
		0.2	2.65	2.56	2.65
		0.4	1.86	1.60	1.85
	0.5 $\phi$	0.0	5.23	5.93	5.93
		0.2	4.09	4.25	4.44
		0.4	2.75	2.32	2.80
	$\phi$	0.0	7.68	13.70	13.70
		0.2	5.98	9.17	9.67
		0.4	3.99	4.22	5.41
40°	0	0.0	5.37	5.39	5.39
		0.2	4.39	4.27	4.39
		0.4	3.34	3.07	3.34
	0.5 $\phi$	0.0	11.66	16.17	16.17
		0.2	9.43	11.99	12.44
		0.4	7.03	7.67	8.63
	$\phi$	0.0	23.22	353.23	353.23
		0.2	18.95	240.62	252.96
		0.4	14.32	127.75	152.52

inclination  $\theta$  and horizontal earthquake acceleration coefficient  $\alpha_h$ . The passive earth pressures obtained by present analysis are found to be higher than those obtained by pseudo-static analysis and much lower than those obtained by assuming a planar failure surface.

**Acknowledgments** The first author wants to acknowledge the partial financial support provided by the Indian Institute of

Technology Kanpur to carry out the present work through a sponsored research project.

## References

- Basha BM, Babu GLS (2009) Computation of sliding displacements of bridge abutments by pseudo-dynamic method. *Soil Dyn Earthquake Eng* 29(1):103–120
- Chang MF (1981) Static and seismic lateral earth pressures on rigid retaining structure. PhD thesis, Purdue University
- Choudhary D, Nimbalkar S (2005) Seismic passive resistance by pseudo-dynamic method. *Geotechnique* 55(9):699–702
- Choudhury D, Nimbalkar S (2007) Seismic rotational displacement of gravity walls by pseudo-dynamic method: Passive case. *Soil Dyn Earthquake Eng* 27(3):242–249
- Choudhury D, Subba Rao KS (2002) Seismic passive resistance in soils for negative wall friction. *Can Geotech J* 39(4):971–981
- Choudhury D, Sitharam TG, Subba Rao KS (2004) Seismic design of earth-retaining structures and foundations. *Curr Sci* 87(10):1417–1425
- Ghosh P (2007) Seismic passive earth pressure behind non-vertical retaining wall using pseudo-dynamic analysis. *Geotech Geol Eng* 25:693–703
- Kramer SL (1996) Geotechnical earthquake engineering. Prentice Hall, New Jersey
- Kumar J (2001) Seismic passive earth pressure coefficients for sands. *Can Geotech J* 38:876–881
- Kumar J, Chitikela S (2002) Seismic passive earth pressure coefficients using the method of characteristics. *Can Geotech J* 39(2):463–471
- Lancellotta R (2007) Lower bound approach for seismic passive earth resistance. *Geotechnique* 57(3):319–321
- Mononobe N, Matsuo H (1929) On the determination of earth pressure during earthquakes. Proc World Eng Conf 9:176
- Nimbalkar S, Choudhury D (2007) Sliding stability and seismic design of retaining wall by pseudo-dynamic method for passive case. *Soil Dyn Earthquake Eng* 27(6):497–505
- Nimbalkar S, Choudhury D (2008) Effects of body waves and soil amplification on seismic earth pressures. *J Earthquake Tsunami* 2(1):33–52
- Okabe S (1926) General theory of earth pressure. *J Jpn Soc Civil Eng* 12(1):311
- Soubra AH (2000) Static and Seismic passive earth pressure coefficients on rigid retaining structures. *Can Geotech J* 37(2):463–478
- Steedman RS, Zeng X (1990) The influence of phase on the calculation of pseudo-static earth pressure on a retaining wall. *Géotechnique* 40(1):103–112
- Subba Rao KS, Choudhury D (2005) Seismic passive earth pressures in soils. *J Geotech Geoenviron Eng ASCE* 131(1):131–135